ANALYSIS OF LAND SUBSIDENCE DUE TO GEOTHERMAL PRODUCTION IN SARULLA GEOTHERMAL FIELD, NORTH SUMATRA, INDONESIA, USING SENTINEL-1

Mochamad Iqbal[1,2,*] and Panggea Ghiyats Sabrian[3]

[1]Petrology, Volcanology, and Geothermal Research Group, Geological Engineering, Institut Teknologi Sumatera, South Lampung, Indonesia.
[2]Graduate School of Engineering, Kyoto University, C1-2, Kyoto Daigaku Katsura, Kyoto, 615-8540, Japan.
[3]Geological engineering, Universitas Mulawarman, Samarinda, East Kalimantan, Indonesia.

*e-mail: mochamad.iqbal@gl.itera.ac.id

Received: 17-01-2023; Revised: 28-06-2023; Approved: 04-08-2023

ABSTRACT. Sarulla geothermal field is one of the largest geothermal fields in the world which has a 330 MW installed capacity. The field consists of three areas, namely Namora Langit (NIL)-1, NIL-2, and Silangkitang (SIL) which operated from 2017 and 2018. It is situated precisely at the Sarulla graben which is an active tectonic area composed of Quaternary Toba tuff and intermediate lava and extrusive felsic pyroclastic Toru. This study aims to see whether land subsidence may emerge in the Sarulla geothermal field and its environments in addition to determining whether the geothermal activity or anthropogenic is responsible for the deformation. We used the persistent scatterer (PS) interferometry synthetic aperture radar (InSAR) method to calculate the rate of subsidence in the area. 30 ascending images from Sentinel-1 were gathered from 5 January to 18 December 2020 with a separation of 12 days to run the analysis. The results demonstrate that Sarulla is undergoing subsidence occurring at NIL-1 and NIL-2 and SIL with a velocity of 0 to -32.9 mm/year. Although negative deformation occurs in the geothermal area, there is no solid evidence indicating geothermal fluid extraction is the cause of subsidence.

Keywords: *geothermal, sarulla, subsidence, PS-InSAR.*

1 INTRODUCTION

The Sarulla geothermal field is located in North Tapanuli Regency, North Sumatra province, Indonesia, which currently has the largest power generation capacity in the world, which is 330MW (Wolf and Gabbay, 2015). It consists of three power plants that generated 110MW each: Silangkitang (SIL) and Namora I Langit (NIL)-1 started their operation in March and October 2017, respectively; meanwhile, NIL-2 began operation on May 2018. The Sarulla geothermal field's exploration already started in 1993 to develop at a maximum of 1000MW (Gunderson et al., 2000).

Geologically, Sarulla is situated at the graben (well known as Sarulla Graben) along the Great Sumatran Fault, the large right strike-slip fault shifting Sumatra Island, extending from north to south (Figure 1), precisely at Toru Segment with a length of 95 km yielded a contractional bend structure (Sieh and Natawidjaja, 2000). Sarulla is adjacent to other geothermal potentials such as low-temperature Tarutung-Sipoholon (Nukman and Hochstein, 2019), Donotasik, and high-temperature Sibual-buali (Gunderson et al., 2000). Based on the geologic map, the NIL area lies at the Toru Volcanic product and Toba tuff, which consist of intermediate lava and extrusive felsic pyroclastic. However, SIL area situated at the Totolan Formation and Young Alluvium. Totolan Formation consists of Pleistocene conglomerate, while the Young Alluvium consists of unconsolidated materials.

SAR (Synthetic Aperture Radar) is a radar that is installed on a plane or artificial satellite. It sends pulse waves to the Earth's surface and collects reflections. D-InSAR (Differential Interferometric SAR) has proven to be an efficient instrument for assessing topographic changes with high spatial resolution across wide areas (Hanseen, 2001). However, the D-InSAR still shows decorrelations caused by DEM, orbitals, atmospheric errors, and other factors. A time series analysis can help to improve D-InSAR accuracy. In InSAR, time series

analysis is utilized to reduce spatial and temporal decorrelation. Using more than two InSAR with the same master results in a duplicate time series method, which is classed as Persistent Scatterer (PS) InSAR (Ferretti et al., 2001).

The main problem focuses on the unexplored potential for ground subsidence in the Sarulla geothermal field, induced by the extensive extraction of geothermal fluids for power generation, which can precipitate substantial geological hazards (Iqbal et al., 2023), such as landslides and surface ruptures, leading to infrastructural damages and potentially, loss of lives (Dai et al., 2001). In geothermal fields, the extraction of fluid leads to a decrease in reservoir pressure, culminating in surface subsidence (Amelung et al., 2000). Notably, the Sarulla geothermal field, the world's largest power generation site, has not been examined for such occurrences. This study, therefore, proposes the utilization of Persistent Scatterer Interferometry Synthetic Aperture Radar (PS-InSAR) technology to detect ground subsidence in the Sarulla geothermal field. PS-InSAR has demonstrated efficacy in monitoring earth surface deformation, particularly in geothermal fields (Aly et al., 2012; Raspini et al., 2022). This technology could provide precise and continuous data concerning ground subsidence, offering an invaluable preventative tool to alleviate larger scale subsidence, akin to those observed in the Taupo Volcanic Zone (Hole et al., 2007). Through the identification and assessment of potential subsidence areas, preventative measures can be implemented to mitigate associated risks, thus ensuring sustainable geothermal operations and the maintenance of regional safety in North Sumatra province, Indonesia.

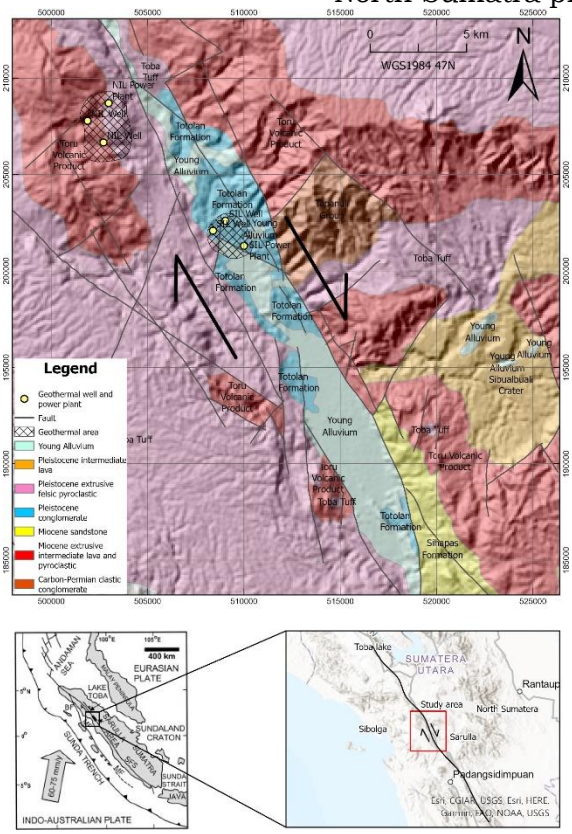

Figure 1-1: Geology of the research area (simplified from Aspden et al., 1982).

2 MATERIALS AND METHODOLOGY

2.1 Location and Data

The research area is situated in Sarulla Geothermal Field, North Tapanuli, North Sumatra. This study utilizes ascending Sentinel-1 data IW (interferometric wide) mode that was retrieved from ESA (European Satellite Agency). About 30 images with a separation of 12 days from 5th January to 18th December 2020 were collected, orbiting at path 142 frame 1184 with polarization VV+VH. Figure 2-1 shows the perpendicular baseline of the satellite

that was used in this research for PS-InSAR processing. This time frame is selected for the study because the Sarulla post-geothermal production deformation will be investigated. Data comparisons between before and after geothermal production should be conducted to optimize the assessment. However, we could only detect deformation based on 2020 data due to time and data limitations.

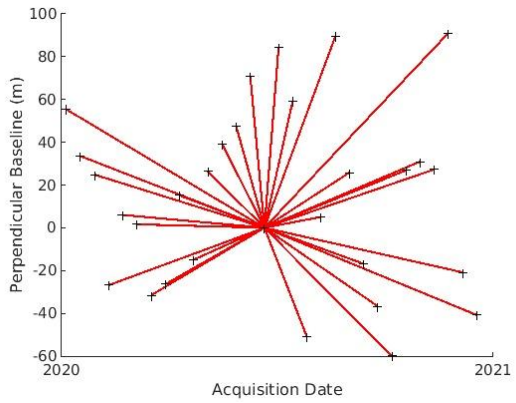

Figure 2-1: Perpendicular baseline of PS-InSAR data used in this research.

2.3 Methods

In this research, we manage to identify the displacement at the Sarulla geothermal field and its surrounding by applying PS-InSAR proposed by (Hooper, 2008; Hooper et al., 2007, 2004). PS pixels are identified from interferograms optimized for PS analysis (Hooper et al., 2007). PS-InSAR achieves a better result than conventional InSAR because it analyzes coherent pixels only with less noise and omits the decoherent. By considering topographic features, signal noise, and environmental influences, PS-InSAR measures land subsidence over the period of a month or year.

The PS-InSAR approach analyzes SAR data time-series. Detailed workflow for this processing is shown in Figure 2-2. The method relies on stable, point-like scatterers that are free of specks and provide a distinct response. These persistent scatterers (PS) provide a consistent phase history over the entire acquisition time range (Ferretti et al., 2001). The PS phases do not demonstrate temporal decorrelation and are stable over time, making it possible to observe and monitor deformation over an extended period of time. The following equation represents the interferometric phase φ_{Int} of the SAR signal of wavelength lambda (λ) between two different images (Khan et al., 2022):

$$\varphi_{Int}=\varphi_{topography}+\varphi_{movement}+\varphi_{orbit}+\varphi_{atmosphere}+\varphi_{noise} \quad (1)$$

where $\varphi_{topography}$ is the phase variation driven on by height errors, $\varphi_{movement}$ is the element generated by terrain displacement in the Line Of Sight (LOS) path in between two SAR acquisitions, φ_{orbit} is the phase error caused by orbit estimate errors, $\varphi_{atmosphere}$ is fluctuations in atmospheric phase delay that affect the phase component. Lastly, φ_{noise} refers to phase noise, including thermal noise and other error components.

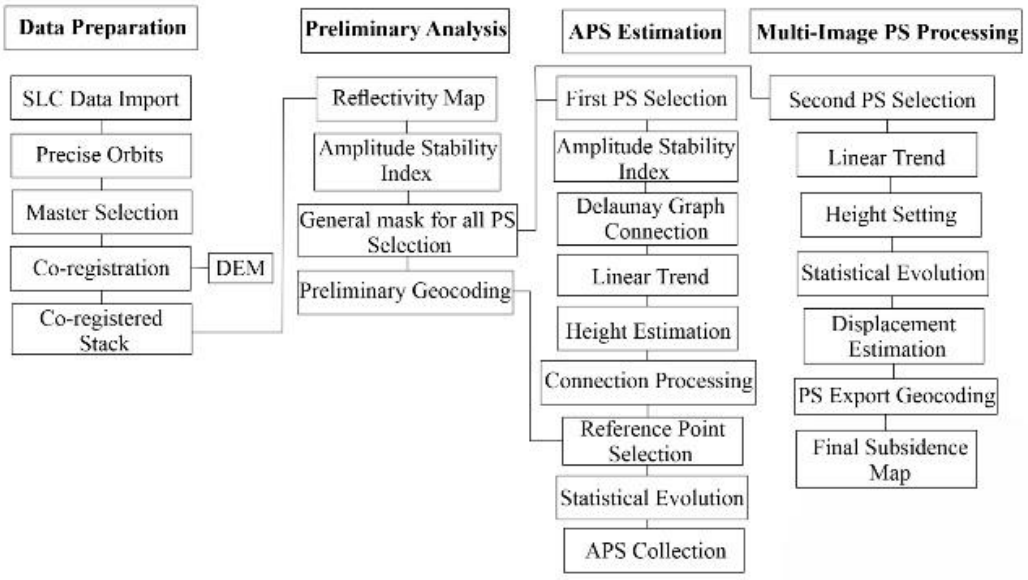

Figure 2-2: PS-InSAR processing workflow (adopted from Khan et al., 2022).

In our study we only look at Line-of-Sight (LOS) direction changes that may be an indication of subsidence and uplift. However, in active tectonic areas, horizontal and vertical movements are very common due to plate movements or faults. The observed LOS changes are compared with the master image acquired on 17 June 2020. The master image was selected by considering the interferogram image that maximizes the sum correlation and minimizes the sum (Hooper et al., 2007).

3 RESULTS AND DISCUSSION

From the results of PS-InSAR processing, we managed to obtain 29 displacement images from each period in comparison to the reference image. Line of sight (LOS) or displacement values ranging from -67 to 50 mm (Figure 3-1). A positive value indicates an uplift while a negative value indicates a subsidence. But more importantly, the results of the PS-InSAR analysis also succeeded in detecting objects around the NIL and SIL geothermal areas which are the main targets as objects that may be directly affected by geothermal production. In addition, PS-InSAR also detects objects around urban areas/main roads located around the Sarulla Graben.

The PS-InSAR method was successful in detecting around 822 PS pixels at NIL and 533 PS pixels at SIL which had LOS <0 mm or subsidence. All the values for these pixels are summarized in Figure 3-2 which contains the average, maximum, and minimum values. It should be noted that the displacement value obtained is the result of a comparison with the reference image. In general, the displacements in NIL and SIL did not indicate a decrease with time; rather, they increased at points and declined at other times, but generally showing slow declining.

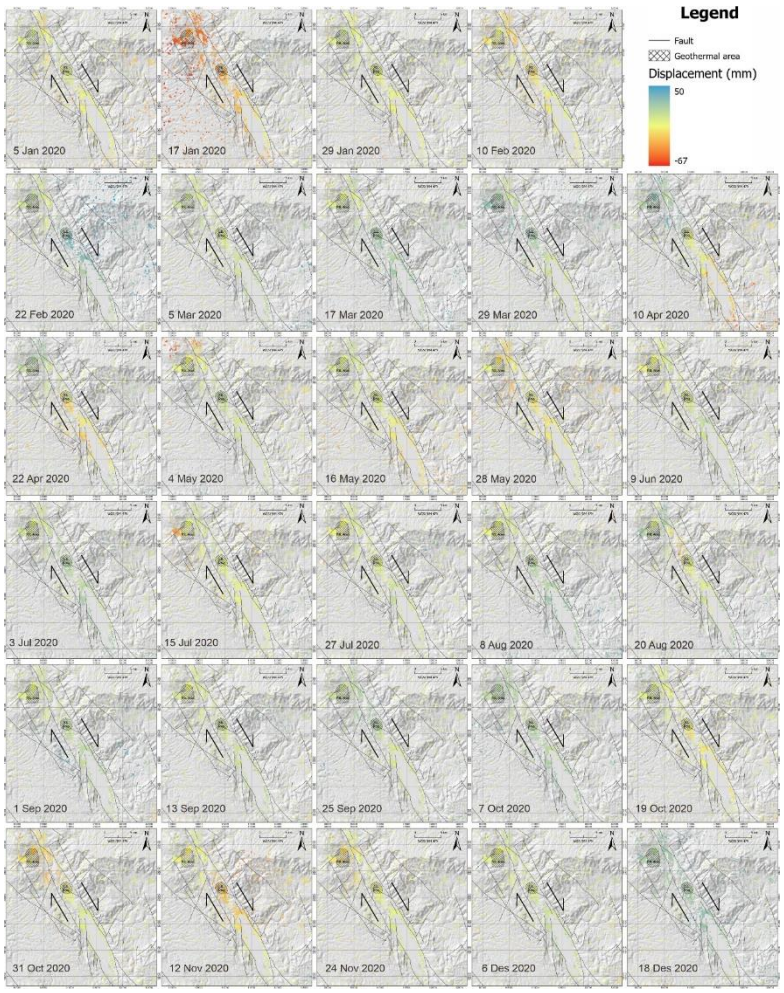

Figure 3-1: Displacement of Sarulla geothermal area and surroundings. The displacement value is compared to the reference satellite image.

Figure 3-2: Summary of displacement in NIL and SIL geothermal area during 2020.

As shown in Figure 3-3, the PS-InSAR analysis findings not only yield displacement data but also the velocity of displacement each year in mm/year. However, since only images from 2020 were used to determine this displacement rate, the value may change if data from other years are included. At Sarulla, the rate of displacement varies from -32.8 to 35.2 mm/year. As can be seen, the geothermal area and the Sarulla graben area contain the objects that have been identified as suffering surface changes.

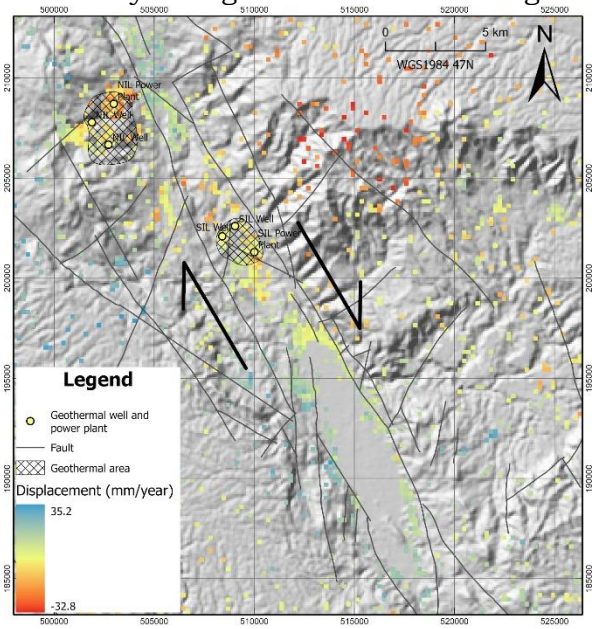

Figure 3-3: Rate of displacement at Sarulla geothermal area and surroundings.

Positive LOS value will be removed from the map in order to only show objects or regions that are undergoing subsidence since this research focuses on this phenomenon. The rate of subsidence in the Sarulla area and its surroundings can be seen in Figure 3-4. The majority of land subsidence occurs in the NIL and SIL areas, which are geothermal production areas consisting of power plants, injection wells, and production wells. In addition, subsidence was also detected outside the NIL and SIL areas. The velocity of land subsidence varies from 0 to 32.9 mm/year.

Figure 3-4 shows a comparison between terrain images (left) and true color composite/TCC (right) in subsidence areas. Buildings, roads, the clearing of new land, and other anthropogenic activities or land uses also have a significant impact on subsidence. It can be observed in the TCC image that many detected objects in the northeastern portion of the study region, which is in a forest area, experience fairly high subsidence. This is presumably

because the PS pixel detects low vegetation or large rock outcrops (Hooper et al., 2007). It is estimated that the region's high subsidence value, which ranges from 19.7 to 32.9 mm/year and is thought to be influenced by local tectonics because the area is adequately distant from geothermal production wells, makes it difficult to conclude that the area's subsidence is directly influenced by Sarulla's geothermal activities. Additionally, it is also supported that the Sarulla Graben is a tectonically active region with a 9 mm/year rate of movement (Hickman et al., 2004).

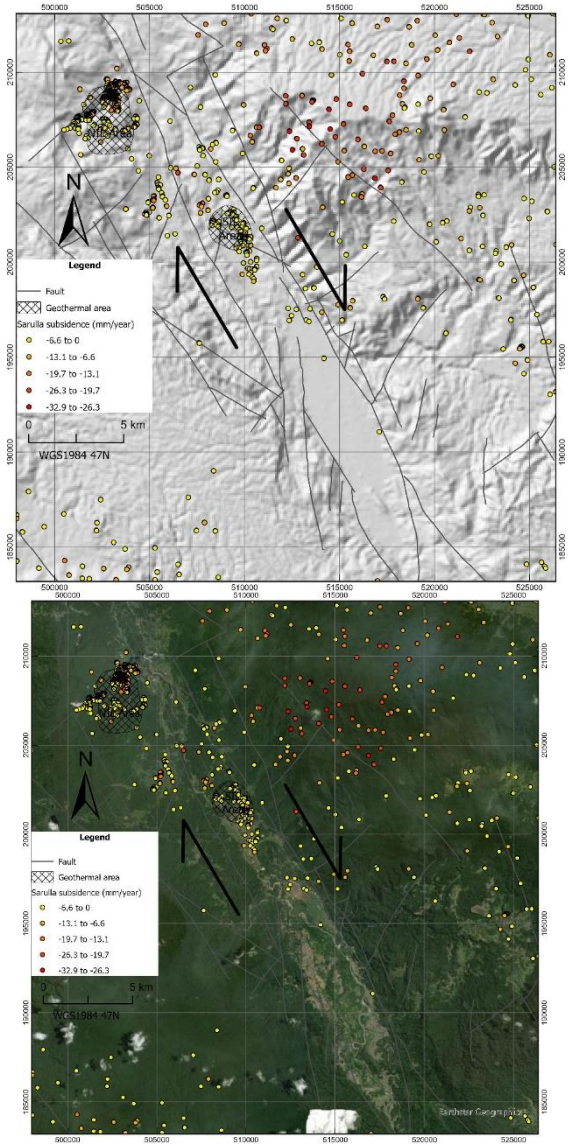

Figure 3-4: Rate of subsidence at Sarulla geothermal area and surroundings. Upper figure shows terrain image and the lower figure is TCC acquired from Landsat 8 OLI/TIRS.

The graphical representation in Figure 3-5 underscores the significant subsidence that is occurring in the NIL geothermal region. Within the scope of this geologically dynamic area, a wide array of objects, detected as Persistent Scatterer (PS) pixels, demonstrate measurable subsidence varying between 6.6 mm to 32.9 mm per annum. The concentration of subsidence is quite marked within the red zone depicted on Figure 3-5. This area encapsulates the geothermal power plant and its immediate environs, exhibiting the highest subsidence rates. It is evident that the exploitation of geothermal resources in this area is affecting the stability of the surface.

The northeastern section of NIL, however, isn't spared from this phenomenon either. It also demonstrates a notable rate of subsidence, which we

attribute to recent construction activities, including building structures and new roadway infrastructure. This observation stresses the potential geological impacts of human activities, extending beyond the immediate vicinity of industrial facilities.

Meanwhile, the blue zone (as delineated in Figure 3-5) signifies an area with less severe but still noteworthy subsidence rates ranging from 6.6 to 13.1 mm per year. These figures correlate with the excavation and construction activities associated with the establishment of power plants in this sector, which has been ongoing since 2017. The fact that the excavation of dump sites for these development projects has resulted in subsidence points towards an unintended environmental consequence of such large-scale operations.

However, it's important to note that the NIL region's geographical isolation from populated settlements mitigates the potential impact of these subsidence rates. Even though a slight degree of sinking is evident, the location's remoteness ensures that the risk of human impact is considerably reduced. Still, it underscores the need for thorough geological evaluations prior to the development of large-scale industrial projects to better anticipate and manage the environmental consequences.

On the contrary, the SIL area, as shown in Figure 3-6, exhibits a much more moderate subsidence rate, ranging from 0 to 6.6 mm per year. Notably, this subsidence is primarily constraint to the geothermal area, specifically around the locations of power plants. Interestingly, even though the geothermal areas are situated in close proximity to a nearby village, no PS pixel, indicative of significant subsidence, is detected in the surrounding residential areas.

This evidence leads us to infer that the geothermal production activities within Sarulla, at least thus far, have not had a direct impact on the settlements lying beyond the immediate operational areas. This finding is significant given the innate vulnerability of geothermal regions to land subsidence, particularly in cases of overproduction. Overexploitation of these geothermal resources can induce land sinking, potentially imposing negative effects on surrounding communities and environments.

A case in point is the Taupo Volcanic Zone in New Zealand, where research Hole et al. (2007) has documented notable land subsidence as a consequence of geothermal activity. There, aggressive geothermal production has resulted in significant land subsidence, disrupting the natural landscape and underscoring the potential ramifications of such activities. Therefore, while the SIL area may not presently show signs of extensive subsidence, continuous monitoring and careful management of geothermal resources are crucial to ensure sustainable operations and minimize potential environmental impacts.

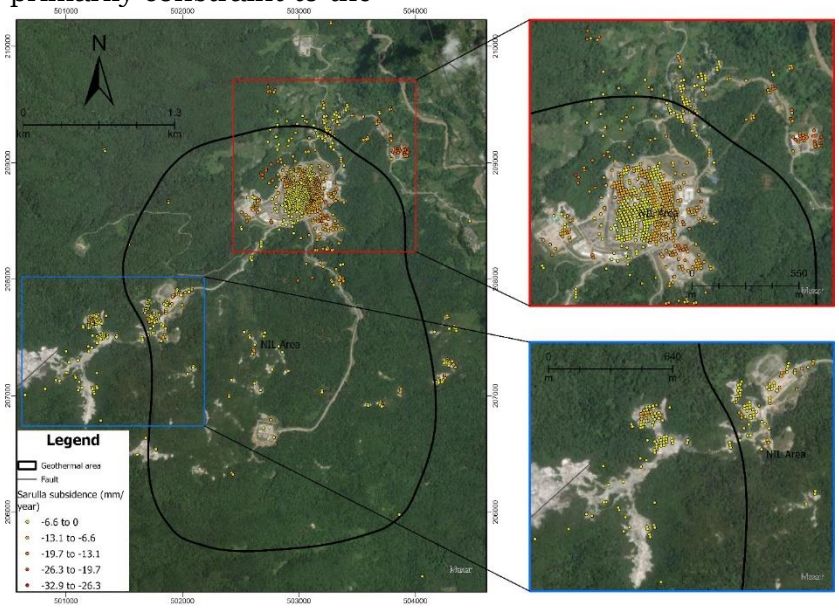

Figure 3-5: Rate of subsidence at NIL area.

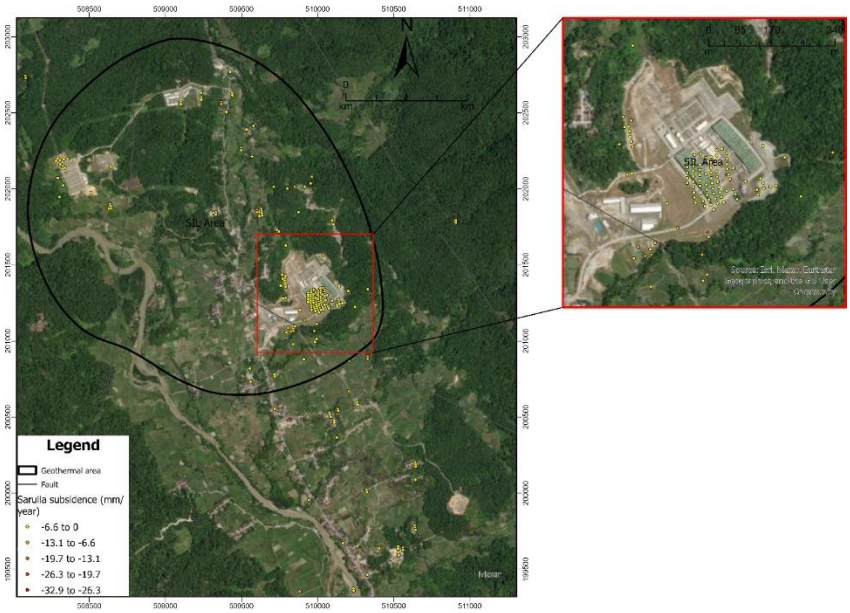

Figure 3-6: Rate of subsidence at SIL area.

4 CONCLUSIONS

With 30 SAR pictures taken in 2020 using the PS-InSAR technique, this study was able to successfully determine the displacement rate that proceeded at Sarulla Geothermal Field and the surrounding area. We can conclude that:

I. Line of sight detected the PS pixel ranging from 35.2 to -32.8 mm/year, which means uplift and subsidence happened in this area. The majority of the positive displacement, which is most likely the result of strike-slip fault activity, is located outside the geothermal area in the Sarulla Graben.

II. Subsidence that occurred in the geothermal area namely NIL and SIL, vary between 6.6 to 32.9 mm/year. Although it comprises a high rate, no further direct evidence that the subsidence is caused by geothermal production. Recent anthropogenic activities such as building and road pavement presumably cause this issue.

III. The geothermal power plant's distant position far (±2 km) from residential areas reduces the risk of subsidence that is tightly correlated to geothermal production which could be impacted the daily local activities.

This study is severely restricted by ground-truthing, a crucial component of remote sensing analysis. Ground checking is essential despite the fact that the PS-InSAR analysis's confidence rate was 68% (Hooper et al., 2007). A PS-InSAR, ground truthing, and GPS measurement combination could improve the results and increase the level of confidence.

ACKNOWLEDGEMENTS

We would like to express our gratitude to the journal editorial team and the reviewers for their help to improve this article.

REFERENCES

Aly, M.H., Klein, A.G., Zebker, H.A., Giardino, J.R., 2012. Land subsidence in the Nile Delta of Egypt observed by persistent scatterer interferometry. Remote Sensing Letters 3, 621–630. https://doi.org/10.1080/01431161.2011.652311

Amelung, F., Jónsson, S., Zebker, H., Segall, P., 2000. Widespread uplift and 'trapdoor' faulting on Galápagos volcanoes observed with radar interferometry. Nature 407, 993–996. https://doi.org/10.1038/35039604

Aspden, J.A., Kartawa, W., Aldiss, D.T., Djunuddin, A., Diatma, D., Clarke, M.C.G., Whandoyo, R., Harahap, H., 1982. Geologic Map of the Padangsidempuan and Sibolga Quadrangles, Sumatra.

Dai, F.C., Lee, C.F., Li, J., Xu, Z.W., 2001. Assessment of landslide susceptibility on the natural terrain of Lantau Island, Hong Kong. Environmental Geology 40, 381–391. https://doi.org/10.1007/s002540000163

Ferretti, A., Prati, C., Rocca, F., 2001. Permanent scatterers in SAR interferometry. IEEE Transactions on Geoscience and Remote Sensing 39, 8–20. https://doi.org/10.1109/36.898661

Gunderson, R., Ganefianto, N., Riedel, K., Sirad-Azwar, L., Sulaiman, S., 2000. Exploration Results in the Sarulla Block, North Sumatra, Indonesia, in: Proceedings World Geothermal Congress. Presented at the World Geothermal Congress 2000, International Geothermal Association, Kyushu-Tohoku, Japan.

Hickman, R.G., Dobson, P.F., Gerven, M. van, Sagala, B.D., Gunderson, R.P., 2004. Tectonic and stratigraphic evolution of the Sarulla graben geothermal area, North Sumatra, Indonesia. Journal of Asian Earth Sciences 23, 435–448. https://doi.org/10.1016/S1367-9120(03)00155-X

Hole, J.K., Bromley, C.J., Stevens, N.F., Wadge, G., 2007. Subsidence in the geothermal fields of the Taupo Volcanic Zone, New Zealand from 1996 to 2005 measured by InSAR. Journal of Volcanology and Geothermal Research 166, 125–146. https://doi.org/10.1016/j.jvolgeores.2007.07.013

Hooper, A., 2008. A multi-temporal InSAR method incorporating both persistent scatterer and small baseline approaches. Geophysical Research Letters 35. https://doi.org/10.1029/2008GL034654

Hooper, A., Segall, P., Zebker, H., 2007. Persistent scatterer interferometric synthetic aperture radar for crustal deformation analysis, with application to Volcán Alcedo, Galápagos. Journal of Geophysical Research: Solid Earth 112. https://doi.org/10.1029/2006JB004763

Hooper, A., Zebker, H., Segall, P., Kampes, B., 2004. A new method for measuring deformation on volcanoes and other natural terrains using InSAR persistent scatterers. Geophysical Research Letters 31. https://doi.org/10.1029/2004GL021737

Iqbal, M., Denhi, A.D.A., Kristianto, Prayoga, A., 2023. Morphological Analysis of Anak Krakatau Volcano after 22 December 2018 Eruption using Differential Interferometry Synthetic Aperture Radar (DInSAR). Journal of Geoscience, Engineering, Environment, and Technology 8, 90–98. https://doi.org/10.25299/jgeet.2023.8.2.11651

Khan, J., Ren, X., Hussain, M.A., Jan, M.Q., 2022. Monitoring Land Subsidence Using PS-InSAR Technique in Rawalpindi and Islamabad, Pakistan. Remote Sensing 14, 3722. https://doi.org/10.3390/rs14153722

Nukman, M., Hochstein, M.P., 2019. The Sipoholon Geothermal Field and adjacent geothermal systems along the North-Central Sumatra Fault Belt, Indonesia: Reviews on geochemistry, tectonics, and natural heat loss. Journal of Asian Earth Sciences 170, 316–328. https://doi.org/10.1016/j.jseaes.2018.11.007

Raspini, F., Caleca, F., Del Soldato, M., Festa, D., Confuorto, P., Bianchini, S., 2022. Review of satellite radar interferometry for subsidence analysis. Earth-Science Reviews 235, 104239. https://doi.org/10.1016/j.earscirev.2022.104239

Sieh, K., Natawidjaja, D., 2000. Neotectonics of the Sumatran fault, Indonesia. Journal of Geophysical Research: Solid Earth 105, 28295–28326. https://doi.org/10.1029/2000JB900120

Wolf, N., Gabbay, A., 2015. Sarulla 330 MW Geothermal Project Key Success Factors in Development. GRC Transactions 39.